EARTH SURFACE PROCESSES AND LANDFORMS, VOL 23, 141–157 (1998)

COARSE BEDLOAD TRANSPORT IN A MOUNTAIN RIVER

P. A. CARLING[1]*, J. J. WILLIAMS[2], A. KELSEY[1], M. S. GLAISTER[3] AND H. G. ORR[1]

[1]*HYSED (Hydrodynamics and Sedimentology Laboratory), Institute of Environmental and Natural Sciences, Lancaster University, Lancaster, LA1 4YB, UK*

[2]*Proudman Oceanographic Laboratory, Bidston Observatory, Birkenhead, Merseyside, LA3 7RA, UK*

[3]*c/o Institute of Freshwater Ecology, Far Sawrey, Ambleside, LA22 0LP, UK*

Received 15 April 1996; Revised 20 March 1997; Accepted 21 May 1997

ABSTRACT

Coarse bedload transport dynamics are investigated utilizing hydrodynamic and sediment transport data obtained in an extensively instrumented study reach located in Squaw Creek, Montana, USA. During 1991 and 1992, a number of discrete bedload transport events associated with the daily rise and fall in stream discharge were investigated. Data show that initiation of sediment transport was accompanied by a reduction in bed roughness and by changes in bulk hydraulic parameters. For larger discharges, coarser fractions of the bed material mobilized, and bedload transport rates and average hydraulic parameters stabilized. As discharge reduced, mobile coarse particles became less frequent and deposited fine particles were removed, resulting in an increase in bed roughness. These observations are attributed to the downstream translation of bar sediments during the passage of a hydrograph. Bedload pulses were aperiodic but spatially variable. Flow turbulence and velocity profile data obtained during low flows allowed comparison between average bed shear stress and apparent bed roughness estimates obtained using different approaches. © 1998 John Wiley & Sons, Ltd.

Earth surf. process. landforms, **23,** 141–157 (1998)
No. of figures: 13 No. of tables: 2 No. of refs: 49
KEY WORDS: mountain river; gravel bedload transport; turbulence; flow resistance; Squaw Creek; Montana

INTRODUCTION

The transport of coarse bedload in steep gravel-bed streams is of practical interest to engineers and hydrologists. Recognition of unsteadiness in bedload transport rates, even during competent flow conditions, has resulted from identification of discrete quasi-periodic bedload 'pulses' (e.g. Solov'ev, 1969; Lekach and Schick, 1983; Ashmore, 1988; Gomez *et al*., 1989; Hoey and Sutherland, 1991). These 'regular' pulses may reflect the development of dynamic bed sediment waves, with length scales equivalent to the channel width (Carson and Griffiths, 1989; Griffiths, 1993), which are associated with scour and fill phenomena (Jackson and Beschta, 1982; Whiting *et al*., 1988). Unsteady transport also occurs at the scale of instantaneous particle interactions with the flow at temporal and spatial scales commensurate with turbulence (e.g. Drake *et al*., 1988; Williams, 1990). However, the downstream translation of unsteady coarse bedload at scales in between these extremes is poorly researched in the field. Gomez (1991) regards 'pulsing' as distinct temporal fluctuations in transport rate which need not be of statistically significant regularity: this definition is adopted herein. Such spatial and temporal organization in bedload may result in subtle temporal changes in bed elevation and bed roughness which may modify local hydraulic conditions (Seminara *et al*., 1996). These changes may then influence bedload dynamics further. Segregation of particles by size may also occur during unsteady transport but this is only well known for temporally well defined pulses (Iseya and Ikeda, 1987; Whiting *et al*., 1988).

Several laboratory studies (e.g. White and Day, 1982; Kuhnle and Southard, 1988) and field data have shown the linkages between the hydraulics and dynamics of sand/fine gravel bedloads (e.g. Drake *et al*., 1988; Whiting *et al*., 1988). In contrast, data pertaining to local hydraulic adjustments during the passage of groups of

* Correspondence to: P. A. Carling
Contract grant sponsor: US Army Corps of Engineers; contract grant number: OAJA-90-C-00006
Contract grant sponsor: NERC
Contract grant sponsor: EC MAST-2 CSTAB Project; contract grant number: MAS2-CT92-0024C

CCC 0197-9337/98/020141–17 $17.50

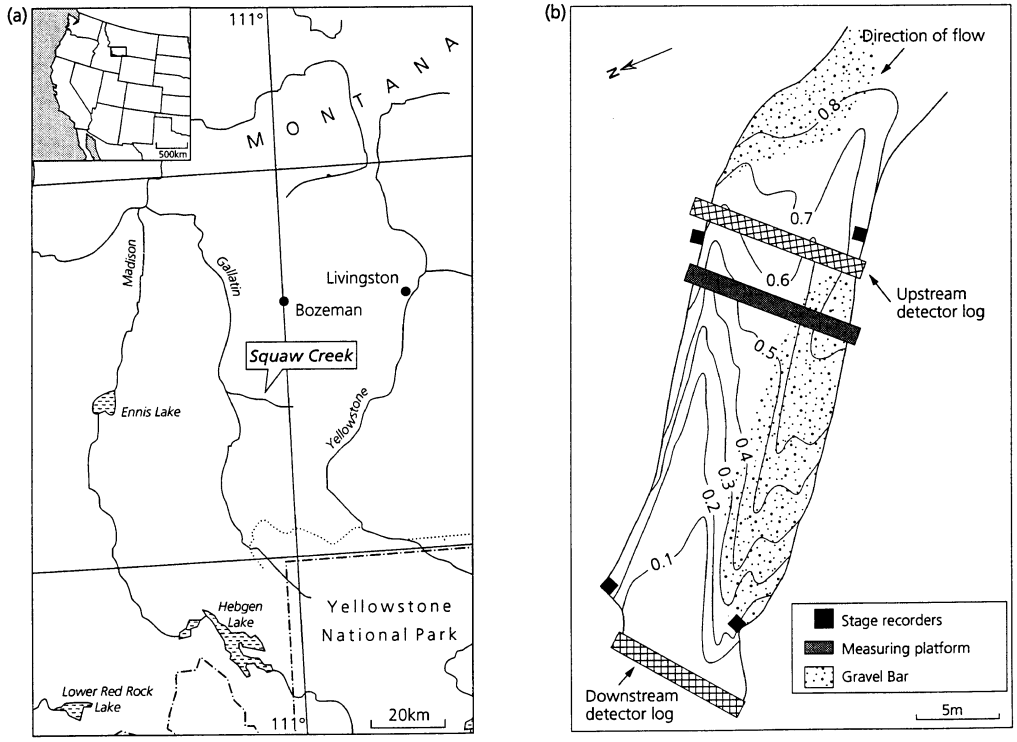

Figure 1. (a) Location of Squaw Creek and (b) plan view of study site

pebbles and cobbles in natural streams are relatively scarce. Preliminary observations on low transport rates of pebbles over static cobble beds (Ergenzinger and Custer, 1982; Spieker and Ergenzinger, 1990) have been made using inductive magnetic detector systems (Ergenzinger and Conrady, 1982; Reid *et al.*, 1984). This paper reports a similar study designed to describe fully the adjustment of river bed and turbulent flow to the unsteady passage of a pebble bedload.

STUDY SITE AND EXPERIMENTS

Squaw Creek (Figure 1a) flows for 22 km through a catchment of 106 km^2 in the Gallatin Range, Montana (McMannis and Chadwick, 1964; Klages *et al.*, 1973). The river reaches its peak annual snowmelt discharge in late May and early June. The peak daily discharge is typically 6 $m^3 s^{-1}$ but may exceed this during spring rainstorms. The bed slope and channel width vary in the ranges 0·02–0·03 and 8–20 m, respectively, and the width:depth ratio in the study reach is 6·7 at bankfull. The 30 m study reach consists of an alternate bar on the left bank and associated main channel with a right-bank bar immediately upstream of the reach (Figure 1b). Median grain sizes (D_{50}) of the bed material range from 24 mm on the bars to 140 mm in the channel where more than 16 per cent of the particles are larger than 200 mm. The bed sediments are well armoured by material greater than D_{50} of bulk samples; that is D_{84} = 90 mm on the bar top and 200 mm in the base of the channel (Table I). This armour is rarely disrupted by flows less than 7 $m^3 s^{-1}$ (Bunte, 1992). Bedload up to 180 mm has been recorded for flows up to bankfull (Bunte, 1992) indicating that the larger elements in the bed sediment form a widely scattered stationary lag.

The natural magnetic properties of the gravel bedload have allowed automated counting of individual particles crossing magnetic detectors at the upstream and downstream limits of the 30 m reach (Figure 1b). The recorded count rates did not exceed the detection limits of the magnetic detectors (MDs) and variation in count rates clearly reflects periods of relatively 'intense' transport and *vice versa*. A purpose-built bridge was used to obtain synoptic hydraulic and topographic data in mid-reach. A typical cross-section of the stream bed, the associated isovels beneath the bridge and the location of MDs are shown in Figure 2.

Table I. Example of particle size distribution of undifferentiated bulk bed-material samples (mm), after Bunte (1996). Particles are ellipsoidal (Bunte, 1996) and fall within the central bladed class of Sneed and Folk (1958)

Position	D_5	D_{16}	D_{25}	D_{50}	D_{75}	D_{84}	D_{95}
Bar	0·4	1·8	5	24	60	90	200
Channel	0·5	2·8	18	140	190	200	220

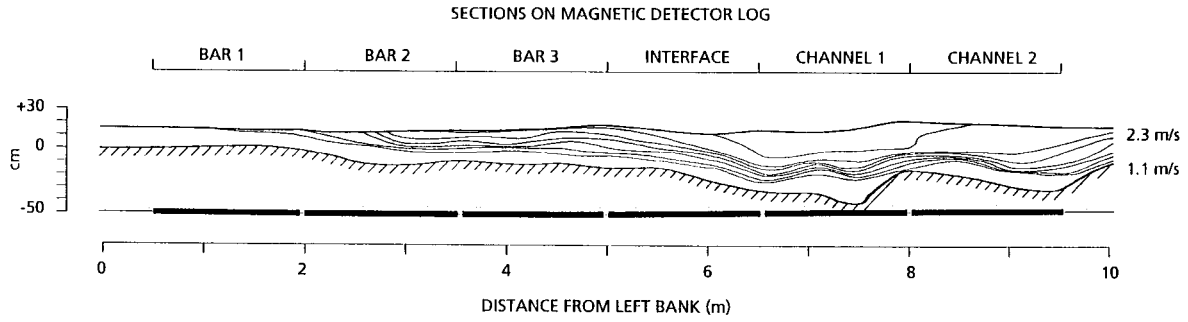

Figure 2. Cross-section of the stream bed beneath sampling platform, flow isovels and the position of the upstream magnetic detector sections

EQUIPMENT AND MEASUREMENTS

Magnetic detection and measurement of bedload transport

The MDs recorded the passage of particles through six 1·5 m spanwise sections across the upstream detector and through five 1·5 m spanwise sections across the downstream detector (Figure 2). Output signals caused by individual magnetic particles in transit were counted, summed and logged using a PC.

Helley-Smith bedload samplers were incapable of trapping cobble bedload. Consequently particles greater than 11 mm were trapped in a net of 1·5 m span, deployed centrally below a sill downstream of the lower detector. The net sampler gave bulk transport rates for periods of about 40 min. The MDs were calibrated over a range of bedload transport rates using net samples. Details of the bedload trap, the MDs calibration procedure and measurement errors are given by Bunte (1992, 1996).

Hydraulic measurements

Four float-operated depth recorders were used to determine water slope, and rapid surveys of bed and water surface elevation relative to a fixed datum were undertaken by lowering rigid vertical rods through a guide-frame fixed to the bridge. Data were obtained at 0·1 m intervals with a vertical resolution of ±0·01 m.

Velocity profiles (1 min integrals) were measured using an array of six OTT C2 current meters at 0·5 m intervals across the channel every hour during the passage of a hydrograph. Additional measurements were made at vertical intervals of 5 mm using an OTT electromagnetic current meter (ECM) (Figure 3). The lowest reading was taken by nestling the sensor between surface bed particles such that zero datum $\cong 0{\cdot}7D_{50}$.

Turbulence was measured and pre-processed as described by Carling *et al*. (1993). A pair of *Valeport* 0·10 m annular ECMs (with 10 Hz filter; Soulsby, 1980) were mounted rigidly at $z = 0{\cdot}24$ m in a flow depth of approximately 1·50 m. The two components of flow in x–z and y–z planes were sampling at 30 Hz for up to 30 min. Velocity profiles were measured adjacent to the ECMs for comparison. The ECMs are not robust and thus it was not possible to obtain data during periods of moderate bedload transport.

Data analysis

Several data sets relating to hydrodynamic conditions and bedload transport rates were obtained but the sediment transport events reported typify others recorded.

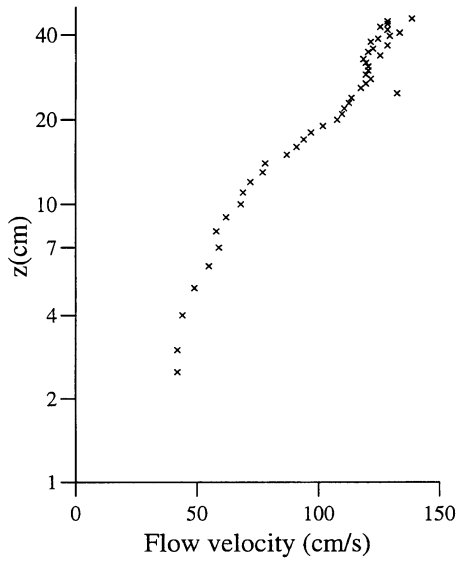

Figure 3. Typical compound velocity profile obtained using the OTT ECM

Table II. Summary of $\overline{U}$, $\overline{U}_{*p}$, $\overline{U}_{*TKE}$, z_{ap}, Cd and z_a values from velocity profile and turbulence data, runs 4–8, June 1993

Run no.	$\overline{U}$ ($cm\,s^{-1}$)	$\overline{U}_{*p}$ ($cm\,s^{-1}$)	$\overline{U}_{*TKE}$ ($cm\,s^{-1}$)	z_{ap} (cm)	Cd $\times10^{-3}$	z_a (cm)
4	133·1	9·2	10·8	0·52	6·6	0·17
5	131·0	8·4	10·1	0·61	5·9	0·13
6	131·2	13·1	12·3	0·79	8·8	0·34
7	125·8	7·9	11·2	0·82	7·9	0·27
8	127·6	14·2	10·7	0·93	7·0	0·20
Av.	129·7	10·6	11·0	0·73	7·2	0·22

If local flow effects are avoided in cobble-bed streams, then results obtained from log-profile analysis in flows with relative depths (D_{50}/d) less than 0·2 can be considered representative of the bulk flow hydraulics (Thorne and Zevenbergen, 1985; Pitlick, 1992; Bathurst, 1993). Estimates of average bed shear velocity ($\overline{U}_{*p}$) and the apparent hydraulic roughness of the bed (z_{ap}) were obtained from velocity log-profile data (subscript p) using:

$$\overline{U}_z = \frac{\overline{U}_{*p}}{k} \ln\left(\frac{z - z_r}{z_{ap}}\right) \tag{1}$$

where $\overline{U}_z$ is the average velocity at a height z above the bed, k is von Kármán's constant (taken to be 0·4) and z_r is the reference height ($0{\cdot}7D_{50}$). Following Wilkinson (1983) only points close to the bed were used to calculate $\overline{U}_{*p}$ and z_{ap} (Table II) using a least-squares regression fit (cf. Bergeron and Abrahams, 1992). In most cases velocity profiles extending to approximately 20 per cent of the depth were found to be approximately logarithmic. Points of inflection from the log-profile indicate the thickness of a constant stress layer associated with the grain roughness (see Figure 3). Above $z \approx 30$ cm, the velocity structure demonstrated greater variance than within the first 20 per cent of the depth. In this respect, velocity profiles indicated the presence of an external boundary layer developed above the highly turbulent flow adjacent to the coarse bed particles. $\overline{U}_{*p}$ and z_{ap} values were generally smaller than the turbulence-derived values (Table II) and exhibited great variation. Further consideration is given to these observations below.

The turbulent streamwise (u'), cross-stream (v') and vertical (w') flow components were obtained following Soulsby *et al.* (1991). Average shear velocity ($\overline{U}_{*TKE}$) was calculated from turbulence data using the turbulent kinetic energy (TKE) approximation (e.g. Soulsby, 1983) using:

$$\frac{\bar{\tau}}{\rho} = \overline{U}^2_{*\mathrm{TKE}} = \xi E \tag{2}$$

where $\bar{\tau}$ is the average bed shear stress, ρ is the density of water, $\xi = 1{\cdot}19$ (Soulsby, 1983), and turbulent kinetic energy E is defined as:

$$E = 0{\cdot}5\left(\overline{u'}^2 + \overline{v'}^2 + \overline{w'}^2\right) \tag{3}$$

A drag coefficient Cd and apparent bed roughness (z_a) at $z = 0{\cdot}24$ m were calculated using:

$$Cd = \overline{U}^2_{*\mathrm{TKE}} / \overline{U}^2_{24} \tag{4}$$

$$z_a = z\mathrm{e}^{\left(-k/Cd^{0{\cdot}5}\right)} \tag{5}$$

where $\overline{U}_{24}$ is the average flow speed $z = 0{\cdot}24$ m. Summary data are given in Table II.

The approximate relationship between z_{ap} (Equation 1), Nikuradse's equivalent roughness (k_s) and a specified grain size for the bed material (D_i) was considered using the general scaling relationship for hydraulically rough streams:

$$k_s = 30z_{ap} \cong \alpha D_i \tag{6}$$

In the absence of large-scale roughness elements, the constant α is often taken to be equal to 3·5 (Hey, 1979; Bray, 1979) when the representative intermediate axis of grains (D_i) is set equal to D_{84} of the planar gravel bed (Table I). The Darcy–Weisbach hydraulic roughness coefficient (f) was calculated using:

$$f = 8\left(\frac{\overline{U}_{*\mathrm{p}}}{\hat{U}}\right)^2 \tag{7}$$

where $\hat{U}$ is the depth-averaged velocity. Unit stream power (ω) and the energy slope (S) of the study reach were calculated using:

$$\omega = \hat{U}\bar{\tau} = \rho g \mathrm{Q}\mathrm{S} / b \tag{8}$$

where average bed shear stress $\bar{\tau} = \rho\overline{U}^2_*$, Q is the discharge and b is the stream width. Section-averaged values of parameters derived using Equations 6–8 were obtained from data integrated across the section.

RESULTS AND DISCUSSION

Theoretical threshold conditions

In common with most field situations, *in situ* determination of average particle threshold shear velocity ($\overline{U}_{*t}$) was not possible at the present site. However, as an aid to interpretation of present data, $\overline{U}_{*t}$ is a useful parameter and a method appropriate for coarse ellipsoidal gravel in shallow streams was used to calculate the theoretical mobility of bed sediments (Carling *et al.*, 1992). Values of $\overline{U}_{*t}$ were calculated for log-normal

velocity profiles, not the frequently observed convex near-bed profiles (e.g. Figure 3). For exposed armour particles seated on shallow cols between co-planar particles $\overline{U}_{*t} = 0{\cdot}27\,\mathrm{m\ s^{-1}}$. For particles constituting the armour layer of the bed, $\overline{U}_{*t} = 0{\cdot}38\,\mathrm{m\ s^{-1}}$. In contrast, mobile gravel moving over the bar in exposed locations ($D_{84} = 60$–$80\,\mathrm{mm}$) requires $\overline{U}_{*t}$ values of at least $0{\cdot}25\,\mathrm{m\ s^{-1}}$ to maintain motion of all grains. Sporadic motion of the finer fraction of bed material (i.e. $D_{50} < 5\,\mathrm{mm}$) would be expected for $\overline{U}_{*t} > 0{\cdot}10\,\mathrm{m\ s^{-1}}$. Use is made below of these theoretical predictions of $\overline{U}_{*t}$.

Hydraulic characteristics and bed sediments

Owing to the paucity of detailed hydrodynamic field data from shallow flows over coarse sediments, the comparability of methods used to determine hydraulic parameters relevant to the study of bedload transport remains uncertain. This section therefore compares hydraulic parameters derived using synoptic profile and ECM data.

For experimental runs 4–8 obtained in June 1993, when the bed remained virtually static, values of $\overline{U}_{*}$ obtained using the TKE and profile methods agree well, but validation of these data remains problematic. However, during acquisition of these data small quantities of 'fine' sediments ($D_{50} \cong 5\,\mathrm{mm}$) were collected in the net and $\overline{U}_{*}$ values in Table II are close to the expected threshold value for the finest fraction of the bed sediments (see above). Consequently, there is corroboration that present $\overline{U}_{*}$ estimates are approximately correct. Further, being derived from separate instruments operating according to different principles, the good agreement between $\overline{U}_{*p}$ and $\overline{U}_{*TKE}$ supports strongly the suggestion that present $\overline{U}_{*}$ estimates are accurate.

Taking the z_{ap} values derived from the velocity profile data (Table II), the equivalent roughness k_s varied between $0{\cdot}156$ and $0{\cdot}279\,\mathrm{m}$, averaging $0{\cdot}22\,\mathrm{m}$, and so $\alpha \cong 1{\cdot}1$ and $2{\cdot}4$ for the channel and bar-top D_{84} sediments, respectively. Obtaining the value of α in accord with observed average k_s values for all spanwise locations gave $\alpha \cong 1{\cdot}7$, a value half that given by Hey (1979) and Bray (1979). This is not surprising as in flows with isolated blocks it is well known that profiles taken below the height of the large-scale roughness underestimate total flow resistance (e.g. Thompson and Campbell, 1979) owing to the omission of the form drag component. In contrast, profile data taken from log-normal segments at $0{\cdot}20\,\mathrm{m} < z < 0{\cdot}40\,\mathrm{m}$ gave a median z_{ap} value of 16 mm (event of 23–24 May 1991) and 18 mm (event of 5–6 June 1991), so that $k_a \cong 2{\cdot}5 D_{84}$ of the channel armour. The higher value of α in the latter case may reflect additional form resistance and is in agreement with the results of Kamphuis (1974) for relative depths (D_{84}/d) of about $0{\cdot}2$.

The Cd and z_a values obtained from ECM data (Table II) are approximately a factor of three times less than z_{ap} values and are smaller than might be anticipated given the large grain size of the bed sediments (Table I). Since the skin friction is governed to a large extent by the physical characteristics of the bed, the reduction in drag implied by these results seemingly arises from a reduction in the form drag component of the total drag with distance above the roughness elements. Since the ECMs were positioned at approximately $0{\cdot}15\,\mathrm{m}$ above the largest particle in the bed it is argued that z_a values reflect the hydraulic roughness of the highly turbulent wake layer adjacent to bed particles and is a phenomenon well documented in flume studies of flow over rough surfaces (e.g. Grass and Mansour-Tehrani, 1995).

Turbulence characteristics

As expected, the statistical distributions of u', v' and w' are found to be approximately Gaussian (e.g. Figure 4a). In contrast, instantaneous stress magnitude ($\tau/\rho = U_*^2$) series derived from instantaneous Reynolds stresses ($u'w'$ and $v'w'$) were positively skewed (e.g. Figure 4b). Further discussion and statistical analyses of these types of distributions are given by Williams *et al*. (1989) and Williams and Tawn (1991). Whilst $\overline{U}_{*}$ values derived using the TKE method were $\cong 0{\cdot}10\,\mathrm{m\ s^{-1}}$, measured peak instantaneous $\overline{U}_{*}$ values exceeded $0{\cdot}30\,\mathrm{m\ s^{-1}}$ (Figure 4b). Despite these high values, most bed particles were observed to remain static. Values of $\overline{U}_{*TKE}$ are close to the expected threshold value for the finer fractions of bed material (see section on *Theoretical threshold conditions*) and so: (1) large instantaneous $\overline{U}_{*}$ values are ineffectual in mobilizing the bed sediments; and/or (2) shelter afforded to the smaller grains at rest between larger particles raises the effective entrainment threshold significantly. Irrespective of the mechanisms, however, these results indicate that average bed shear stress is an appropriate parameter to use to describe the threshold condition in coarse-bedded shallow streams.

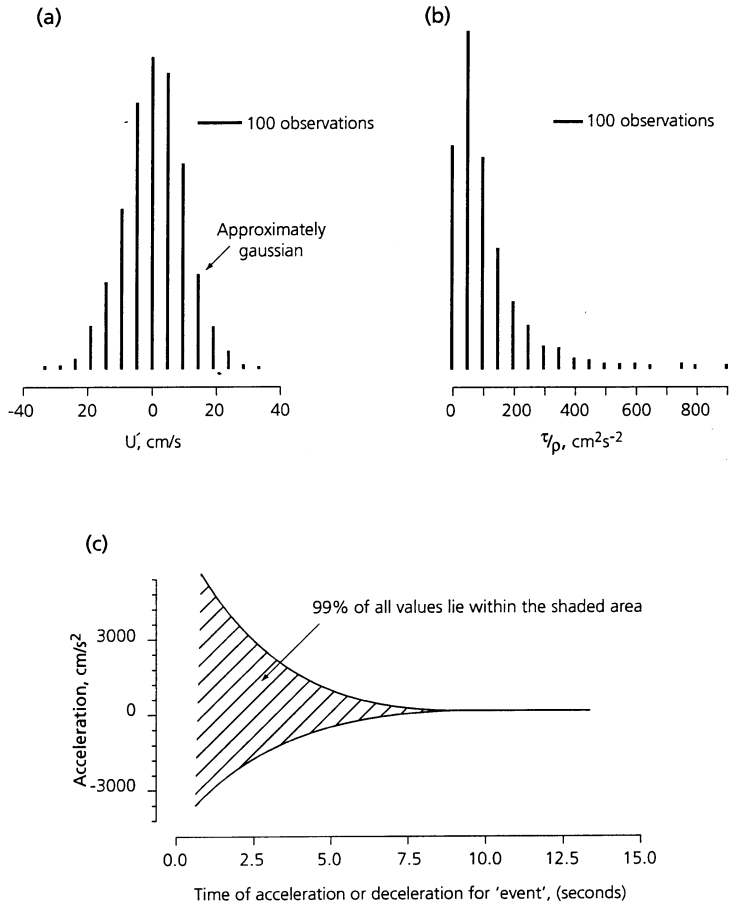

Figure 4. (a) Histogram of instantaneous u' values from a typical flow record; (b) histogram of instantaneous stress magnitude (τ/ρ) values; and (c) acceleration/de-acceleration values associated with near-bed flow

Instantaneous changes in velocity (e.g. Figure 4c) demonstrate that bedload particles are subjected to rapid, high-magnitude flow accelerations and de-accelerations through time. In view of the low rates of sediment recruitment described above, the rapid, high-magnitude near-bed pressure fluctuations did not play a significant role in grain entrainment from the armour layer.

The standard deviation of individual 10 min portions of ECM data taken from an uninterrupted 1·5 h period showed no significant low-frequency modulation (less than 10 mm s^{-1}) through time. This result is in contrast to the low-frequency energy peaks (5–10 min) associated with flow over large sandy bedforms (Lapointe, 1992, 1993).

Using spectral and autocorrelation analyses (Williams *et al.*, 1989), typical turbulent eddy length scales for u', v' and w' were found to be approximately 0·52 m, 0·54 m and 0·11 m, respectively. These data indicate that typical eddies at $z = 0{\cdot}24$ m scale with flow depth rather than with the size of roughness elements on the bed and support further the argument that the present measurements were obtained above the wake region adjacent to bed particles.

Bedload transport dynamics

Typical bedload count data (b_c) across the section, both for bedload entering and leaving the reach, show considerable fluctuations in the number of particles in motion (Figure 5). Within an individual hydrograph, structure in b_c indicative of a statistically significant pulsing phenomenon is absent and there is little correlation

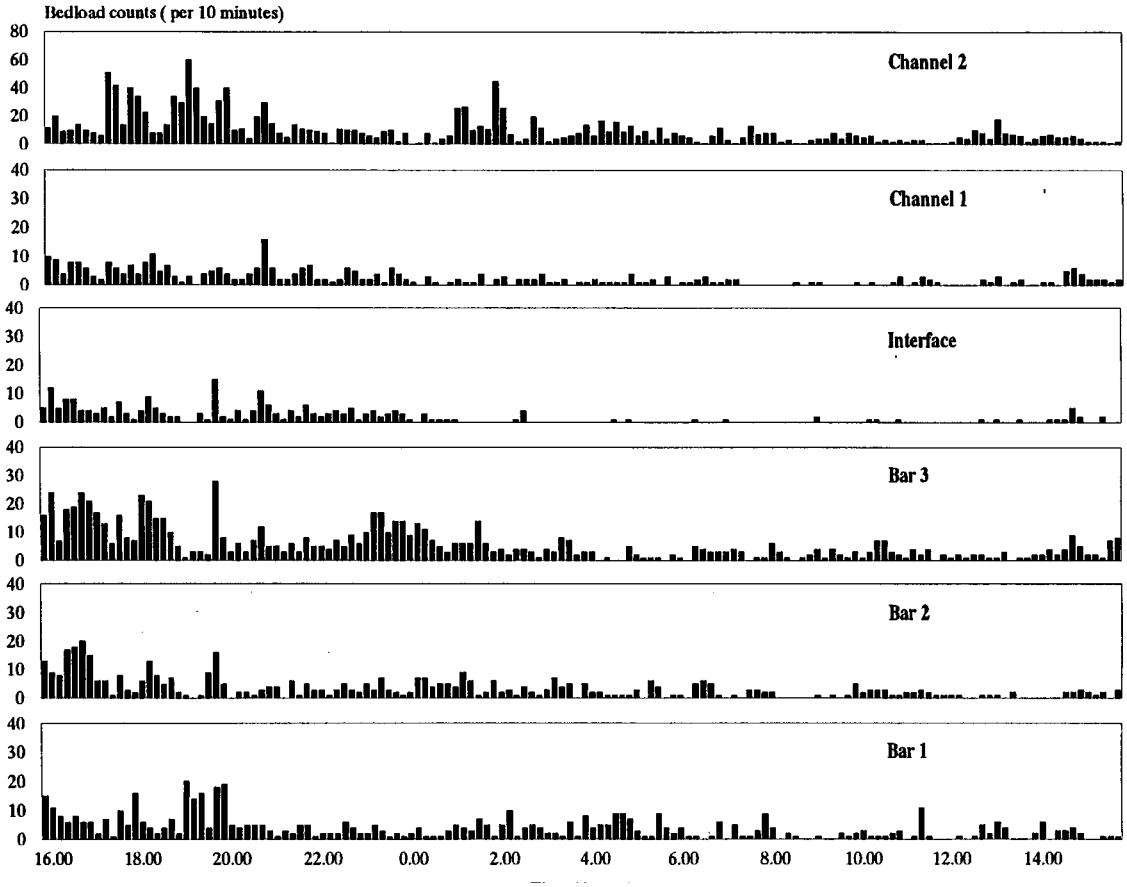

Figure 5. Example of detector counts (per 10 min) at specified spanwise locations for event of 23–24 May 1991

with $\overline{U}_*$, f, d, Q or ω, irrespective of the data record considered (see Figures 11 and 12). This observation indicates that bedload transport during individual hydrographs is essentially aperiodic (although spatially coherent) driven by turbulent fluctuations in bed shear stress, vagaries of individual particle entrainment and the random break-up of discrete particle clusters (e.g. Reid *et al.*, 1984; Williams and Tawn, 1991).

To examine spatial and temporal variability in bedload transport further, b_c series obtained at locations across the channel were examined spectrally. Irrespective of location, b_c spectra were broadly similar (Figure 6) and were characterized by a single significant peak at a frequency of 10^{-4} cycles min^{-1} corresponding to the daily periodicity in the snowmelt hydrographs (cf. Bunte, 1992). The smaller peaks in spectral energy density occurring at approximately 0·02, 0·03 and 0·04 cycles min^{-1} (Figure 6) were found to be statistically random.

In laboratory studies at various temporal scales, bedload transport rates have been shown to be approximately normally distributed (McClean and Tassone, 1987; Gomez *et al.*, 1989):

$$f(t_q) = \left[1/(2\pi)^{0.5}\right] e^{-t_q^2/2} \tag{9}$$

For b_c data from the present study, normalized bedload counts, t_q are defined as:

$$t_q = (b_c - \bar{b}_c)/\sigma \tag{10}$$

where b_c and $\bar{b}_c$ are section count rate and the average section count rate, respectively, and σ is the standard

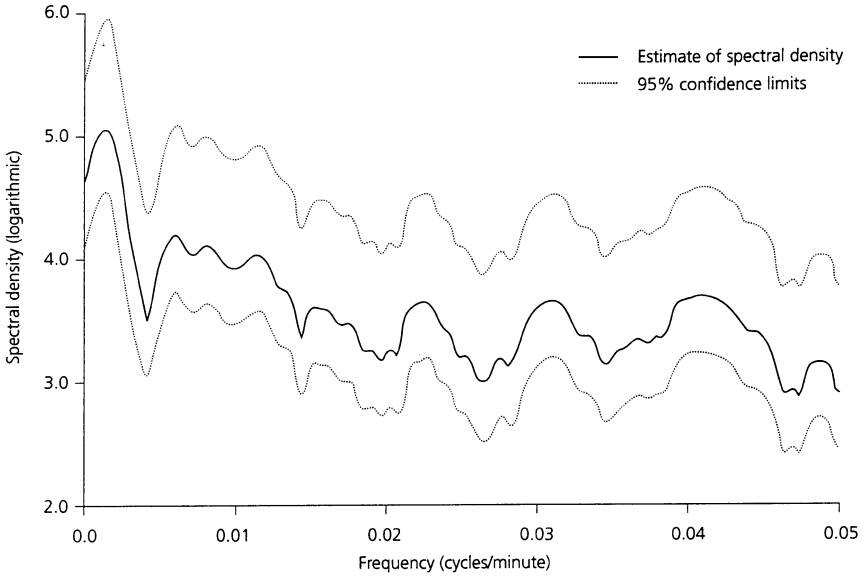

Figure 6. Spectral signature (solid line) and 90 per cent confidence intervals (dashed lines) for detector counts on the bar top for the bedload transport event on 5–6 June 1991

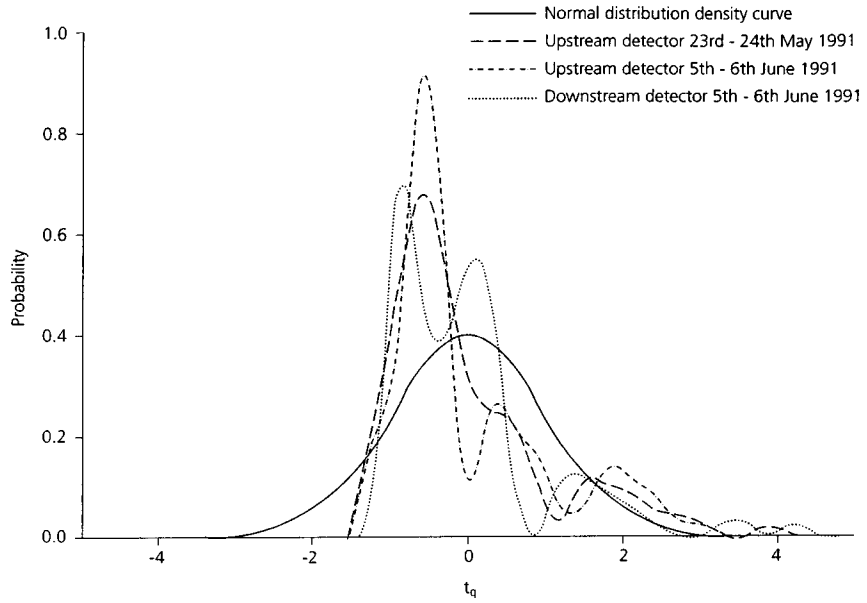

Figure 7. Probability distributions for channel-wide detector counts compared with the normal distribution for events of 23–24 May and 5–6 June 1991

deviation of b_c. Similarity in the peakedness and the degree of skew of smoothed probability density functions (PDFs) for t_q at different spanwise and upstream/downstream sample locations and for different transport events imply that bedload transport was essentially self-similar irrespective of location (Figure 7). At the present spanwise spatial resolution of 1·5 m there was no evidence that the coarse bedload moved in distinct transverse bands characterized by 'high' and 'low' transport rates (cf. Bathurst *et al.*, 1986; Warburton, 1992). Although maximum b_c values were measured in the channel, the whole stream width became active once bedload motion began.

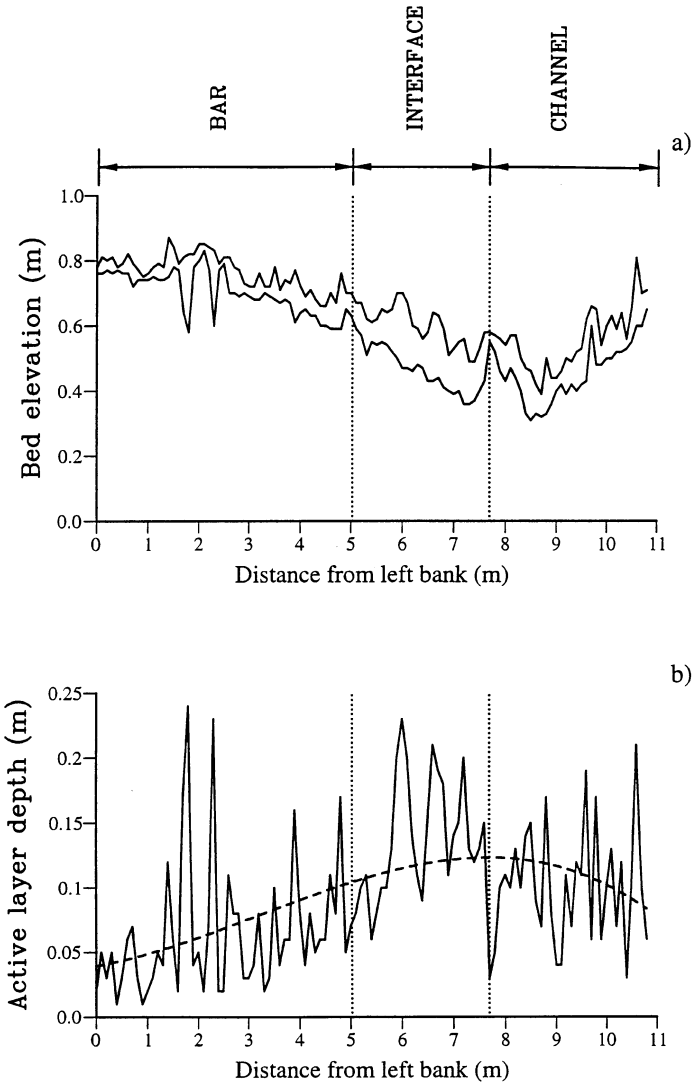

Figure 8. Bedload transport event of 23–24 May 1991: (a) maximum and minimum bed elevation; (b) minimum thickness of active layer

Changes in hydraulic roughness

If net erosion or deposition of sediment occurs during the passage of bedload through the study reach, there should be accompanying changes in bed elevation. This was investigated by measuring differences in the level of the bed during periods of active bedload transport. At each spanwise sample point, the minimum bed-level elevations were subtracted from the maxima (Figure 8a) to provide a measure of the minimum thickness of the mobile layer (Figure 8b). The changes in bed elevation approximately 2 m from the left bank represent events which are spatially and temporally isolated and are not considered further. The maximum changes in elevation, equivalent to one or two armour particle diameters, were observed to occur along the interface between the bar and the channel (Figure 8b). This area showed the most variation in bed elevation throughout the duration of the event.

Following Hoey and Sutherland (1991), temporal changes in bed elevation were examined by considering the standard deviation (σ_ε) of the bed-level records obtained during two bedload transport events. Here, σ_ε is used as a statistic to express the temporal changes in the physical roughness of the bed, where high and low values of σ_ε

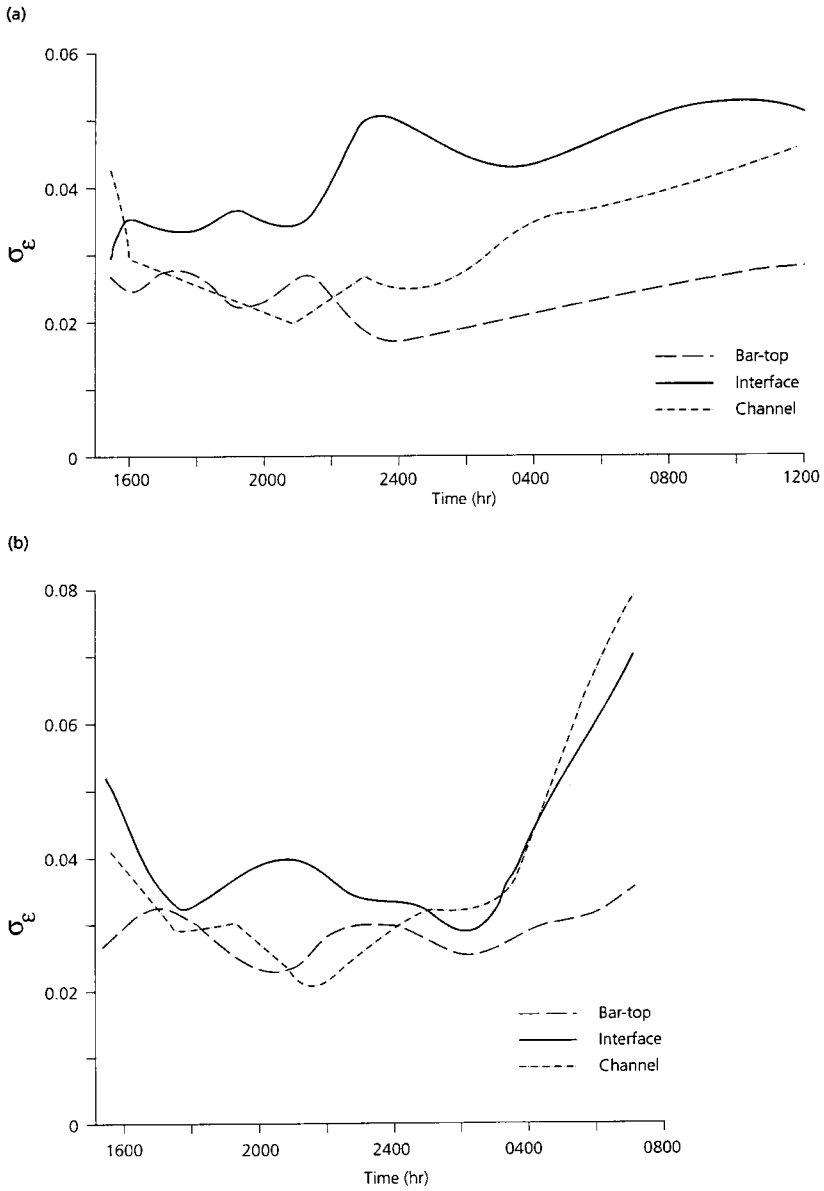

Figure 9. Smoothed bed-level standard deviation (σ_ε) at specified spanwise locations during bedload transport events of (a) 23–24 May and (b) 5–6 June 1991 (smoothing function is $0{\cdot}25x_{i-1}+0{\cdot}5x_i+0{\cdot}25x_{i+1}$)

correspond to physically rough and smooth beds, respectively. Variations in smoothed σ_ε values for bedload transport events on 23–24 May and 5–6 June 1991 are shown in Figures 9a and 9b, respectively. In both these cases and others, σ_ε values were observed to be more variable at the interface area than at the bar top or the channel locations. Figure 9 also shows that as σ_ε values increase at the interface there is a corresponding decrease in σ_ε values at the bar top and *vice versa*. As bedload transport commences and q_b exceeds $2\,g\,m^{-1}\,s^{-1}$, σ_ε values are observed to decline slightly and thereafter fluctuate only slightly irrespective of q_b values. Following the passage of a bedload event there is an increase in σ_ε values and a corresponding decrease in D_{max} of the mobile population. Together these observations indicate that an initially rough stream bed becomes smoother during transport of bedload sediments and subsequently returns to a rough condition when bedload transport ceases. Further consideration of this phenomenon is given below.

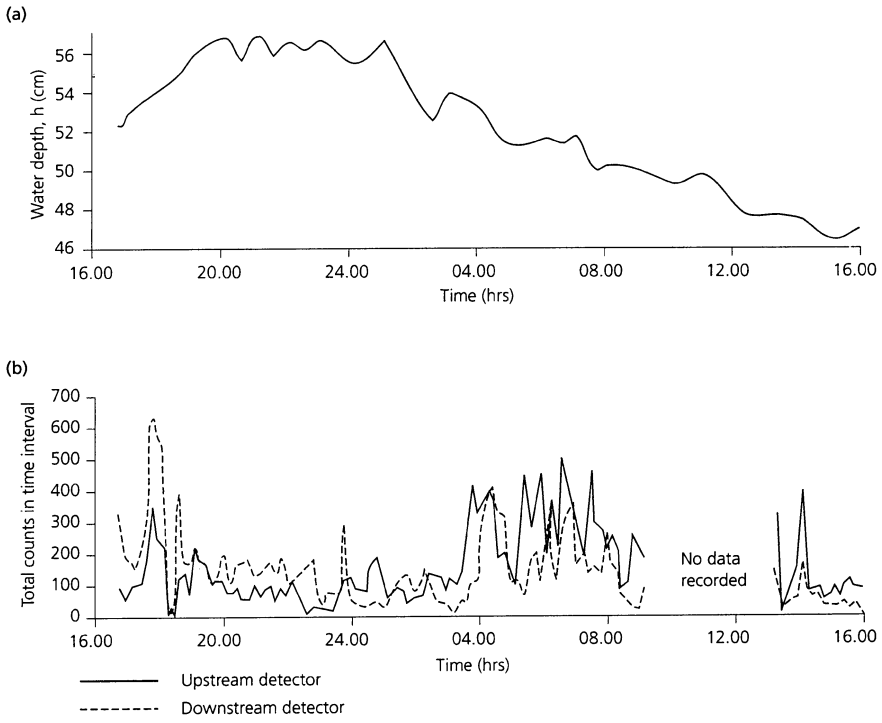

Figure 10. (a) Variation in river stage and (b) detector count data at upstream and downstream locations, 23–24 May 1991

Bedload transport event characteristics

When taken as a complete record, the input and output of particles to and from the study reach recorded by the MDs are approximately balanced (a typical example spanning 1400 min is shown in Figure 10). During rising stage (Figure 10a), however, input and output of particles were observed to be unbalanced with approximately twice as many particles leaving the reach as entering. Peaks in b_c at the upstream and downstream detectors were nearly coincident (Figure 10b) and correlation between peaks in the b_c record and temporal changes in discharge were not detected. During falling stage (Figure 10a), input and output of bedload was also unbalanced. In this regime a net input of bed material into the reach was recorded and cross-correlation demonstrated that downstream b_c peaks lagged upstream b_c peaks by up to 50 min. Correlations between peaks and minima in b_c series recorded during falling stage at the upstream and downstream MD sites, however, were less clear than those evident at the start of the record.

It appears, therefore, from the evidence presented above, that the transport of bedload in Squaw Creek is neither steady nor simply linked to stage. To model the general relationship between input and output of bed materials in the study reach, a general statistical transfer function (Young, 1984; Young and Brenner, 1990) was used to predict a downstream b_c series using the appropriate upstream b_c record. Figures 11a and 11b show stage and an observed downstream b_c series together with the corresponding b_c record predicted by the transfer function. Statistically significant cross-correlations between observed and predicted b_c series indicate strong spatial coherence in coarse bedload transport through the study reach (Figure 11b) and support further the interpretation of the observations presented above.

Bedload and bulk hydraulic parameters

Section-integrated data in Figure 12 show temporal trends in q_b and the hydraulic parameters $\bar{\tau}$, f, d, Q and ω for two transport events. Choosing the event of Figure 12a as a typical example, it can be seen that although discharge tended to decrease after 20:00 h, the passage of a bedload event through the reach at approximately 22:00 h led to an observed reduction in $\bar{\tau}$, f, d and ω (Figure 12a). Similar reductions in bed roughness were

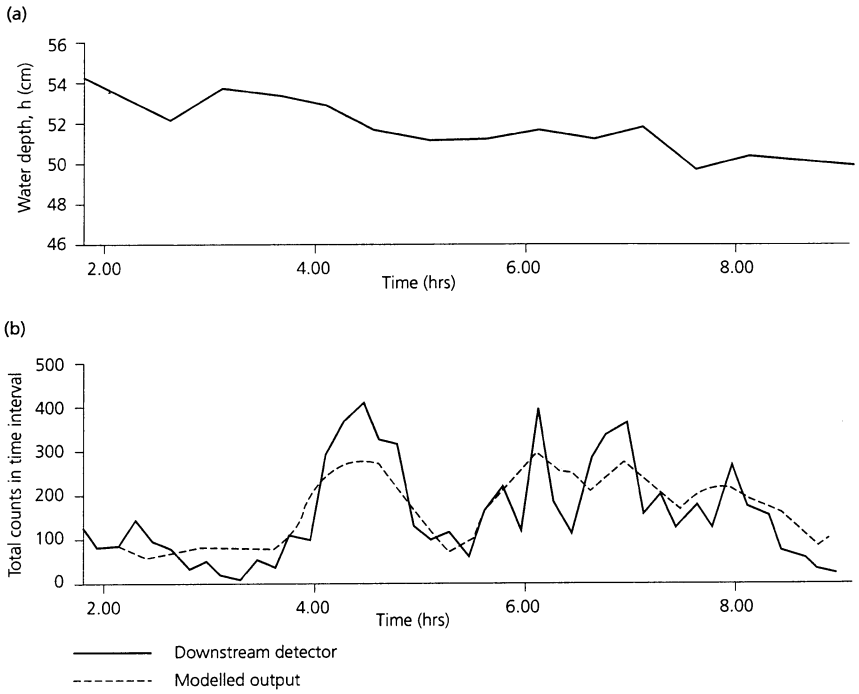

Figure 11. (a) Variation in river stage and (b) comparison between transfer function predictions and observed bedload counts at the downstream location, 23–24 May 1991

associated with bedload transport during three other monitored events (e.g. Figure 12b). Following the passage of the bedload event, f increased, and the parameters $\bar{\tau}$, d and ω readjusted. These observations, showing smoothing and roughening of the river bed during the passage of a bedload event, support the interpretation of particle count data above.

Changes in D_{50} and the maximum particle size (D_{max}) in bedload samples occurred during all monitored events. For example, for 23–24 May 1991 (Figure 12a) bedload was at first (16:00 h) dominated by finer gravel with a negligible percentage coarser than 84 mm but temporal variations in D_{50} were small. At approximately 17:00 h the distribution coarsened slightly. As argued above (confirmed by limited visual observations of the bed), it is considered that coarsening resulted from a loss of fines which previously had become entrapped between pockets in the static armour. There was then little subsequent change in the distribution until 02:00 h. By 03:00 h bedload transport over the bar decreased in response to falling stage and finer gravel previously entrapped between the static armour increasingly dominated the distributions. As a result, the coarse fraction declined steadily from <127 mm to <45 mm, with only sporadic examples of cobbles in transport after 09:00 h. Subsequent sporadic transport of cobbles and fines recorded between 08:00 h and 12:00 h were related to readjustment of bed particles in response to new local hydraulic conditions.

Changes in flow resistance

It is often considered that low rates of sediment transport in coarse-gravel rivers have an insignificant effect on flow resistance (e.g. Bathurst, 1993), primarily because little momentum is extracted from the flow. However, the physical smoothing or roughening of the bed demonstrated above should not be neglected. Therefore when the intensity of transport is low, and the armour is largely intact, fixed-bed resistance equations are unlikely to be applicable. This hypothesis was tested by applying Hey's (1979) flow resistance equation to the data for the bedload transport events of 23–24 May and 5–6 June 1991, when bedload transport was relatively weak:

$$(8/f)^{0{\cdot}5} = 5{\cdot}75 \log(aR/3{\cdot}5D_{84}) \tag{11}$$

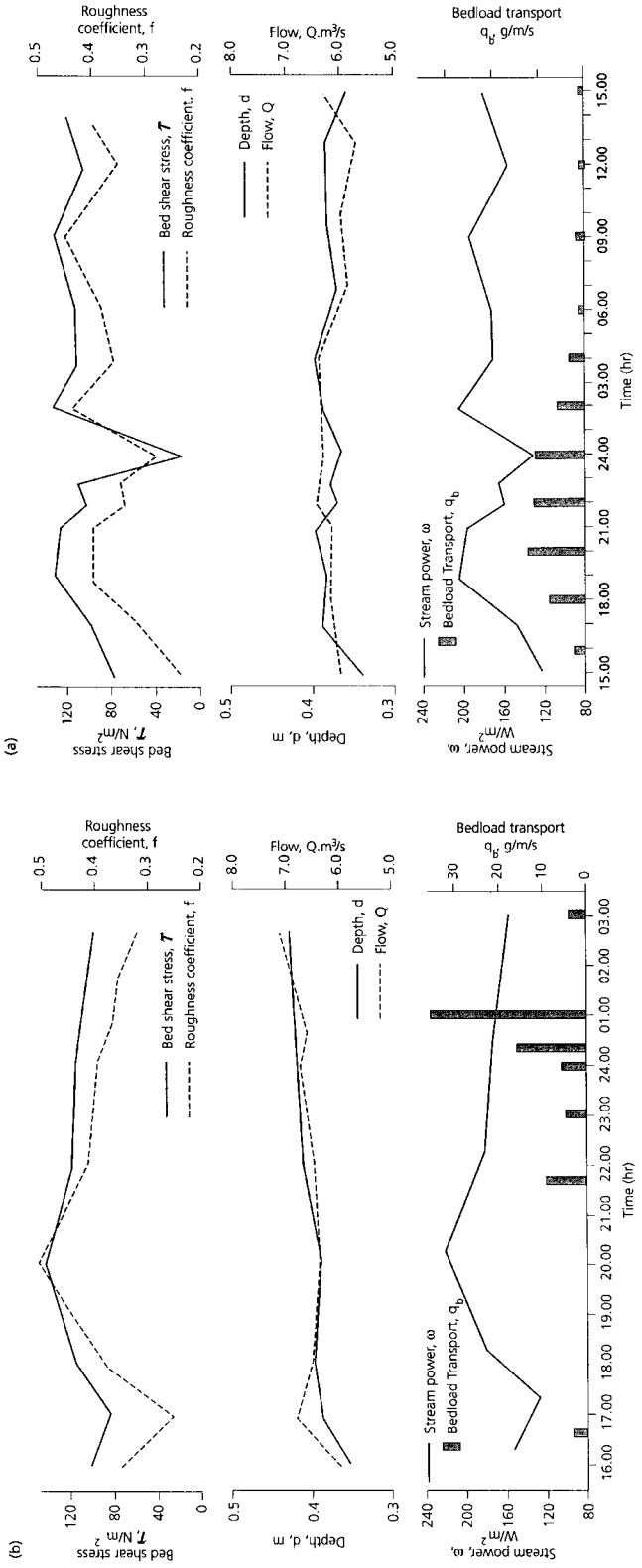

Figure 12. Variation in bulk flow parameters τ, f, d, Q, ω and b_c for events of (a) 23–24 May 1991 and (b) 5–6 June 1991

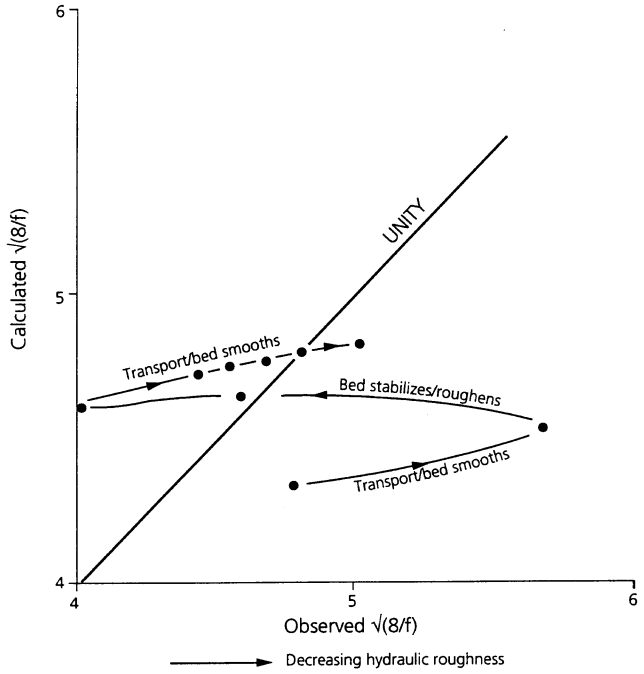

Figure 13. Comparison of observed and calculated bed roughness for event of 5–6 June, with and without bedload transport

Here a is a constant and R is the hydraulic radius. In gravel-bed rivers Hey's equation generally compares well with measured flow resistance over stable beds (Bathurst, 1993). In using Equation 11, it was assumed that for a broad shallow channel (Hey, 1979), $a = 11{\cdot}1$. For conditions of zero transport, D_{84} should take a constant value. However, this value is not known with certainty and thus it was optimized to provide the most favourable fit for Equation 11. This was achieved by first substituting observed values of R and f into the equation to produce a range of values for D_{84}. When $(8/f)$ is calculated incorporating a constant value of D_{84} and an observed variation in flow depth, the inadequacy of the fixed-bed function becomes apparent. As sediment transport commenced, the observed hydraulic roughness of the bed decreased and observed values of $(8/f)$were much larger than predicted by Equation 11 (Figure 13). As bedload transport reduced, observed and predicted $(8/f)$ values initially were found to converge. As bedload transport reduced still further the hydraulic roughness continued to increase and diverge significantly from calculated $(8/f)$ values. When transport commenced again after 21:00 h, $(8/f)$ values again showed an increasing trend as river hydraulics adjusted to the new boundary conditions imposed by mobile sediments.

SYNTHESIS OF OBSERVATIONS

When taken together, measurements of stream bed elevation, sediment budget and particle size provide evidence of processes associated with the downstream translation of coarse bed sediments during moderate flow events. Since sediments constituting the bars are significantly finer than channel sediments (Table I) and channel sediments are heavily armoured, the upstream bars must be the principal source of sediment supplied to the channel during a moderate bedload transport event. At low stage, these sediments are observed to be above the water level and to remain static. As stage rises, they become entrained and are transported downstream. The smoothing of the bed reported above results from infilling of the coarse channel grain interstices by the finer particles in transit. In such situations, $\overline{U}_*$ remains well above the $\overline{U}_{*t}$ value for the finer particles and grains at rest between coarser ones are re-entrained and subsequently replaced rapidly as bedload translates downstream. Available evidence suggests that the channel armour remains essentially undisturbed. With falling stage, the source of finer particles is no longer exposed and $\overline{U}_*$ values fall at all locations. Whilst the entrainment rate of fine particles from the bars is reduced, the stream still retains sufficient energy to mobilize the finer fractions of

the channel sediments and these continue to be transported downstream. As a net result, the channel-bed sediments are observed to coarsen. It is considered that the finer sediment fractions continue downstream until they encounter a low-energy bar environment where they are deposited to await transportation during the passage of the next competent hydrograph.

ACKNOWLEDGEMENTS

Thanks are extended to Professors P. Ergenzinger and G. Christaller (Berlin), Dr K. Bunte (University of Colorado), and Professor S. Custer and Big Timber Works Incorporated and Hogin Machine and Welding (Montana). Funding by the US Army Corps of Engineers (Contract DAJA45-90-C-00006), NERC and the EC MAST-2 CSTAB project (Contract MAS2-CT92-0024C) is gratefully acknowledged. The comments of anonymous reviewers considerably improved the presentation of results.

REFERENCES

Ashmore, P. E. 1988. 'Channel morphology and bedload pulses in braided, gravel-bed streams', *Geografiska Annaler,* **73A**(1), 37–52.

Bathurst, J. C. 1993. 'Flow resistance through the channel network', in Beven, K. and Kirkby, M. J. (Eds), *Channel Network Hydrology,* John Wiley and Sons, Chichester, 69–98.

Bathurst, J. C., Leeks, G. J. L. and Newson, M. D. 1986. 'Field measurements for hydraulic and geomorphological studies of sediment transport – the special problems of mountain streams', in Wessels, A. C. E. (Ed.), *Measurement Techniques in Hydraulic Research,* Balkema, Rotterdam, 137–151.

Bergeron, N. and Abrahams, A. 1992. 'Estimating shear velocity and roughness length from velocity profiles', *Water Resources Research,* **28**, 2155–2158.

Bray, D. 1979. 'Estimating average velocity in gravel-bed rivers', *Journal of the Hydraulic Division ASCE,* **105**, 1103–1122.

Bunte, K. 1992. 'Particle number grain-size composition of bedload in a mountain stream', in Billi, P., Hey, R. D., Thorne, C. R. and Tacconi, P. (Eds), *Dynamics of Gravel Bed Rivers,* John Wiley and Sons, Chichester, 55–68.

Bunte, K. 1996. *Analyses of the Temporal Variation of Coarse Bedload Transport and Its Grain Size Distribution,* General Technical Report RM-GTR-288, USDA Forest Service, Fort Collins, 123 pp.

Carling, P. A., Kelsey, A. and Glaister, M. S. 1992. 'Effect of bed roughness, particle shape and orientation on initial motion criteria', in Billi, P., Hey, R. D., Thorne, C. R. and Tacconi, P. (Eds), *Dynamics of Gravel Bed Rivers,* John Wiley and Sons, Chichester, 23–40.

Carling, P. A., Williams, J. J., Glaister, M. G. and Orr, H. G. 1993. *Particle Dynamics and Gravel-Bed Adjustments,* Unpublished Final Technical Report, Contract No. DAJA45-90-C-00006, European Research Office of the US Army, London, 46 pp.

Carson, M. A. and Griffiths, G. A. 1989. 'Gravel transport in the braided Waimakariri River: mechanisms, measurements and predictions', *Journal of Hydrology,* **109**, 201–220.

Drake, T. G., Shreve, R. L., Dietrich, W. E., Whiting, P. J. and Leopold, L. B. 1988. 'Bedload transport of fine gravel observed by motion-picture photography', *Journal of Fluid Mechanics,* **192**, 193–217.

Ergenzinger, P. and Conrady, J. 1982. 'A new tracer technique for measuring bedload in natural channels', *Catena,* **9**, 77–80.

Ergenzinger, P. and Custer, S. 1982. 'First experiences measuring coarse material bedload transport with a magnetic device', in *Euromech 156, Mechanics of Sediment Transport,* 223–227.

Gomez, B. 1991. 'Bedload transport', *Earth Science Reviews,* **31**, 89–132.

Gomez, B., Naff, R. L. and Hubbell, D. W. 1989. 'Temporal variations in bedload transport rates associated with the migration of bedforms', *Earth Surface Processes and Landforms,* **14**, 135–156.

Grass, A. J. and Mansour-Tehrani, M. 1995. 'Generalised scaling of coherent bursting structures in the near-wall region of turbulent flow over smooth and rough boundaries', in Ashworth, P. J., Bennett, S. J., Best, J. L. and McClelland, S. J. (Eds), *Coherent Flow Structures in Open Channels: origins, scales and interactions with sediment transport and bed morphology,* John Wiley & Sons, Chichester, 41–61.

Griffiths, G. A. 1993. 'Sediment translation waves in braided gravel-bed rivers', *Journal of Hydraulic Engineering,* **119**(8), 924–937.

Hey, R. D. 1979. 'Flow resistance in gravel bed rivers', *Journal of the Hydraulic Division, ASCE,* **105**(HY4), 365–379.

Hoey, T. B. and Sutherland, A. J. 1991. 'Channel morphology and bedload pulses in braided rivers: a laboratory study', *Earth Surface, Processes and Landforms,* **16**, 447–462.

Iseya, F. and Ikeda, H. 1987. 'Pulsations in bedload transport induced by a longitudinal sediment sorting: a flume study using sand and gravel mixtures', *Geografiska Annaler,* **69**A, 15–27.

Jackson, W. L. and Beschta, R. L. 1982. 'A model of two-phase bedload transport in an Oregon coast range stream', *Earth Surface Processes and Landforms,* **7**, 517–527.

Kamphuis, J. W. 1974. 'Determination of sand roughness for fixed beds', *Journal of Hydraulic Research,* **12**, 193–203.

Klages, M. G., Logan, L. D. and Hsieh, Y. P. 1973. 'Suspended solids carried by the Gallatin River of South West Montana I. Amounts carried during spring run off', *NorthWest Science,* **47**, 203–212.

Kuhnle, R. A. and Southard, J. B. 1988. 'Bedload transport fluctuations in a gravel bed laboratory channel', *Water Resources Research,* **24**, 247–260.

Lapointe, M. F. 1992. 'Burst-like sediment suspension events in a sand bed river', *Earth Surface Processes and Landforms,* **17**, 253–270.

Lapointe, M. F. 1993. 'Monitoring alluvial sand suspension by eddy correlation', *Earth Surface Processes and Landforms,* **18**, 157–175.

Lekach, J. and Schick, A. P. 1983. 'Evidence for transport of bedload waves: analysis of fluvial sediment samples in a small upland stream channel', *Catena,* **10**, 267–279.

McClean, D. G. and Tassone, B. 1987. 'Discussion of bed load sampling and analysis', in Thorne, C. R., Bathurst, J. C. and Hey, R. D. (Eds), *Sediment Transport in Gravel Bed Rivers*, John Wiley and Sons, Chichester 109–113.
McMannis, W. J. and Chadwick, R. A. 1964. 'Geology of the Garnet Mountain Quadrangle, Gallatin County, Montana', *Montana Bureau of Mines and Geology Bulletin*, **43**, 47.
Pitlick, J. 1992. 'Flow resistance under conditions of intense gravel transport', *Water Resources Research*, **28**, 891–903.
Reid, I., Brayshaw, A. C. and Frostick, L. E. 1984. 'An electromagnetic device for automatic detection of bedload motion and its field applications', *Sedimentology*, **31**, 269–276.
Seminara, G., Colombini, M. and Parker, G. 1996. 'Nearly pure sorting waves and the formation of bedload sheets', *Journal of Fluid Mechanics*, **312**, 253–278.
Sneed, E. D. and Folk, R. L. 1958. 'Pebbles in the lower Colorado River, Texas a study in particle morphogenesis', *Journal of Geology*, **66**, 114–150.
Solov'ev, N. Y. 1969. 'Pulsation of the movement of bedload in mountain streams', *Trudy GGI*, **175**, 119–123.
Soulsby, R. L. 1980. 'Selecting record length and digitising rate for near-bed turbulence measurements', *Journal of Physical Oceanography*, **10**, 208–219.
Soulsby, R. L. 1983. 'The bottom boundary layer of shelf seas', in Johns, B. (Ed.), *Physical Oceanography of Coastal and Shelf Seas*, Elsevier, 189–266.
Soulsby, R. L., Goldberg, D. G. and Stevenson, E. C. 1991. *Norfolk Sand Banks. Analysis of STABLE data*, HR Wallingford Report No. **EX 2345**, 18 pp.
Spieker, R. and Ergenzinger, P. 1990. *New developments in measuring bedload by the magnetic tracer technique. Erosion, transport and deposition processes*, IAHS Publication No. **189**, 169–178.
Thompson, S. M. and Campbell, P. L. 1979. 'Hydraulics of a large channel paved with boulders', *Journal of Hydraulic Research*, **17**, 341–354.
Thorne, C. R. and Zevenbergen, L. W. 1985. 'Estimating mean velocity in mountain rivers', *Journal of Hydraulic Engineering, ASCE*, **111**, 612–624.
Warburton, J. 1992. 'Observations of bedload transport and channel bed changes in a proglacial mountain stream', *Arctic and Alpine Research*, **24**, 195–203.
White, W. R. and Day, T. J. 1982. 'Transport of graded gravel bed material', in Hey, R. D., Bathurst, J. C. and Thorne, C. R. (Eds), *Gravel Bed Rivers*, John Wiley and Sons, Chichester, 181–223.
Whiting, P. J., Dietrich, W. E., Leopold, L. B., Drake, T. G. and Shreve, R. L. 1988. 'Bedload sheets in heterogeneous sediment', *Geology*, **16**, 105–108.
Wilkinson, R. H. 1983. 'A method for evaluating statistical errors associated with logarithmic velocity profiles', *Geo-Marine Letters*, **3**, 49–52.
Williams, J. J. 1990. 'Video observations of marine gravel transport', *Geo-Marine Letters*, **10**, 157–164.
Williams, J. J. and Tawn, J. A. 1991. 'Simulation of bedload transport of marine gravel', in *Speciality Conference, WRDA Coastal Sediments 1991 Proceedings*, 703–716.
Williams, J. J., Thorne, P. D. and Heathershaw, A. D. 1989. 'Comparison between acoustic measurements and predictions of the bedload transport of marine gravel', *Sedimentology*, **36**, 973–979.
Young, P. C. 1984. *Recursive Estimation and Time Series Analysis: Introduction*, Springer-Verlag, Berlin.
Young, P. C. and Brenner, S. 1990. *MicroCAPTAIN Handbook Version 2.0*, Centre for Research on Environmental Systems, Institute of Environmental and Biological Sciences, Lancaster.

